

# Mechanism of Decomposition of Nitroaromatics. Laser-Powered Homogeneous Pyrolysis of Substituted Nitrobenzenes

Alicia C. Gonzalez,<sup>†</sup> C. William Larson,<sup>‡</sup> Donald F. McMillen,\* and David M. Golden

Department of Chemical Kinetics, Chemical Physics Laboratory, SRI International, Menlo Park, California 94025 (Received: December 26, 1984)

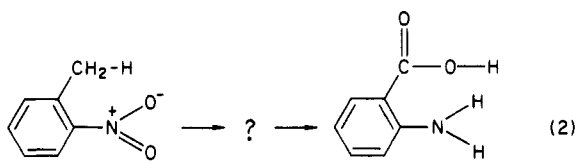
Laser-powered homogeneous pyrolysis (LPHP) has been used to study the gas-phase thermal decomposition of nitrobenzene (NB), *m*-dinitrobenzene (*m*-DNB), *p*-nitrotoluene (*p*-NT), *o*-nitrotoluene (*o*-NT), and 2,4-dinitrotoluene (2,4-DNT) under conditions where surface-catalyzed reactions are precluded. The Arrhenius parameters have been determined by comparative rate measurements relative to cyclohexene decomposition and the reaction mechanisms have been established. In all cases, the rate-limiting step is the homolysis of the Ar-NO<sub>2</sub> bond. The measured Arrhenius parameters for homolysis range from  $\log A = 14.5$  to  $16.4$  and  $E_a$  from  $67.0$  to  $70.0$  kcal/mol. The C-NO<sub>2</sub> bond dissociation energies (kcal/mol) and values of  $\log k$  (s<sup>-1</sup>) for NB, *m*-DNB, *p*-NT, *o*-NT, and 2,4-DNT have been derived from these results and are as follows:  $71.4 \pm 2.0$ ,  $(15.5 \pm 0.5) - (68.2 \pm 1.7)/2.3RT$ ;  $73.2 \pm 2.4$ ,  $(14.5 \pm 0.5) - (70.0 \pm 2.1)/2.3RT$ ;  $71.4 \pm 2.3$ ,  $(14.9 \pm 0.5) - (68.2 \pm 2.0)/2.3RT$ ;  $70.2 \pm 2.5$ ,  $(16.4 \pm 0.6) - (67.0 \pm 2.2)/2.3RT$ ;  $70.6 \pm 2.0$ ,  $(15.3 \pm 0.4) - (67.4 \pm 1.7)/2.3RT$ .

## Introduction

The thermal decomposition of aromatic nitrocompounds has received considerable attention from chemists over the last 50 years, but the reported<sup>1</sup> Arrhenius parameters cover a wide range and the products of the initial steps are essentially unknown. It is well-known<sup>2</sup> that the thermal decomposition of nitrobenzene in a N<sub>2</sub> carrier stream results in biphenyl and other products traceable to initial bond scission to form phenyl radical and NO<sub>2</sub>, but *o*-nitrotoluene reacts under these same conditions by a different pathway.<sup>3</sup> In the latter case, the principal product has been shown to be aniline, resulting from the initial formation of anthranilic acid.<sup>3</sup> Similarly, the presence of an *o*-methyl, -amino, or -hydroxy substituent has been reported<sup>4</sup> to cause a shift in the Arrhenius parameters for gas-phase decomposition from those expected for thermolysis of an approximately 70 kcal/mol bond to values suggestive of a complex intramolecular process:



$$\log k_d (\text{s}^{-1}) = (17.0 - 69.0)/2.303RT$$



$$\log k_d (\text{s}^{-1}) = (12.4 - 49.5)/2.303RT$$

Although various six-membered transition states leading to the intramolecular redox reaction shown in reaction 2 are geometrically quite plausible, none of them appear to lead directly to sufficiently stable products to be associated with the observed activation energy: OH elimination has been suggested<sup>4</sup> as the first step, but this reaction as written is estimated<sup>5</sup> to be 80 kcal/mol endothermic, and therefore could not give rise to an activation energy in the range of 40 kcal/mol. On the other hand, the stable products observed in reaction 2 require substantial movement of at least four atoms, a kind of rearrangement that is difficult to imagine taking place in a single elementary step in the gas phase. These results lead us to suggest that the complex reactions indicated by the reaction products and the unexpectedly low Arrhenius parameters were due to surface-catalyzed reactions, notwithstanding efforts made to avoid them. This would be consistent with various condensed-phase TNT studies that have

suggested through spectroscopic observations<sup>6</sup> or isotope effects<sup>7</sup> that the initial reaction(s) do involve the *o*-methyl group.

Preliminary experiments in which very low-pressure pyrolysis (VLPP) was used to study the decomposition of 2,4-dinitrotoluene also provide rates consistent with a low *A* factor and low activation energy process ( $\log k_d$  (2,4-DNT) (s<sup>-1</sup>) =  $(12.1 - 43.9)/2.3RT$ ), and not indicative of thermolysis of the Ar-NO<sub>2</sub> bond.<sup>8</sup> Since in VLPP all substrate heating is by contact with the reactor walls, surface-catalyzed reactions can dominate in substrates that are prone to them. Therefore, various coatings were used on the VLPP reactor in attempts to eliminate such reactions, but ultimately what appeared to be a surface-catalyzed reaction could not be eliminated. Thus these results were consistent with, but did not prove, our speculation that the low Arrhenius parameters previously reported were due to surface reactions.

We have developed a pulsed-laser technique in which a CO<sub>2</sub> laser is used to indirectly heat the substrate via an absorbing but unreactive gas (e.g., SF<sub>6</sub>). During and after the laser heating of the SF<sub>6</sub>, rapid vibrational-to-vibrational energy transfer occurs between SF<sub>6</sub> and the bath and sample molecules. Under these conditions, there is no surface component to the reactions, since the wall remains cold relative to the reaction temperature. After

(1) (a) Dacons, J. C.; Adolph, H. G.; Kamlet, M. J. *J. Phys. Chem.* **1970**, *74*, 3035. (b) See, for example: Maksimov, Y. Y. *Russ. J. Phys. Chem.* **1972**, *46*, 990. Dubovitskii et al. *Ibid.* **1961**, *35*, 148. (c) Beckmann, J. W.; Wilkes, J. J.; McGuire, R. P. *Thermochem. Acta* **1977**, *19*, 111.

(2) Hand, C. W.; Merritt, Jr., C.; DiPietro, C. *J. Org. Chem.* **1977**, *42*, 841.

(3) (a) Fields, E. K.; Meyerson, S. *Tetrahedron Lett.* **1968**, *10*, 1201. (b) Fields, E. K.; Meyerson, S. *Adv. Free-Radical Chem.* **1965**, *5*, 101.

(4) (a) Matveev, V. G.; Dubikhin, V. V.; Nazin, G. M. *Inst. Khim. Fiz. Chronologovka, USSR* **1978**, *4*, 783. (b) Matveev, V. G.; Dubikhin, V. V.; Nazin, G. M. *Acad. Sci., USSR Bull., Div. Chem. Sci.* **1978**, *2*, 474 and references cited therein.

(5) (a) Benson, S. W. "Thermochemistry and Chemical Kinetics", 2nd ed.; Wiley: New York, 1976. (b) McMillen, D. F.; Golden, D. M. *Annu. Rev. Phys. Chem.* **1982**, *33*, 493-532. (c) Batt, L.; Robinson, G. N. In "Chemistry of Functional Groups - Supplement F"; Patai, S., Ed.; Wiley: Chichester, UK, 1981; p R1035.

(6) (a) Davis, L. P.; Turner, A. G.; Carper, W. R.; Wilkes, J. S.; Dorey, R. C.; Pugh, H. L.; Siegenthaler, K. E. 181st National Meeting of the American Chemical Society, Atlanta, Ga, March-April 1981; American Chemical Society: Washington, DC, 1981. (b) Sharma, J.; Owens, F. J. *J. Chem. Phys. Lett.* **1979**, *61*, 280. Owens, F. J.; Sharma, J. *J. Appl. Phys.* **1980**, *51*, 1494. (c) Davis, L. P.; Turner, A. G. *Int. J. Quantum Chem.* **1983**, *17*, 193. (d) Turner, A. G.; Davis, L. P. *J. Am. Chem. Soc.* **1984**, *106*, 5447. (e) Davis, L. P.; Turner, A. G.; Carper, W. R.; Wilkes, J. S.; Dorey, R. C.; Pugh, H. L.; Siegenthaler, K. E. "Thermochemical Decomposition of TNT: Radical Identification and Theoretical Studies"; Frank J. Seiler Research Laboratory, Project Report FJSRL TR-81-0002, April 1981.

(7) Shackelford, S. A.; Beckman, J. W.; Wilkes, J. S. *J. Org. Chem.* **1977**, *42*, 4201.

(8) McMillen, D. F., unpublished work.

<sup>†</sup> Visiting Scientist on leave from Consejo Nacional de Investigaciones Cientificas de la Republica Argentina.

<sup>‡</sup> Currently at Rocket Propulsion Laboratory, Edwards Air Force Base, CA.

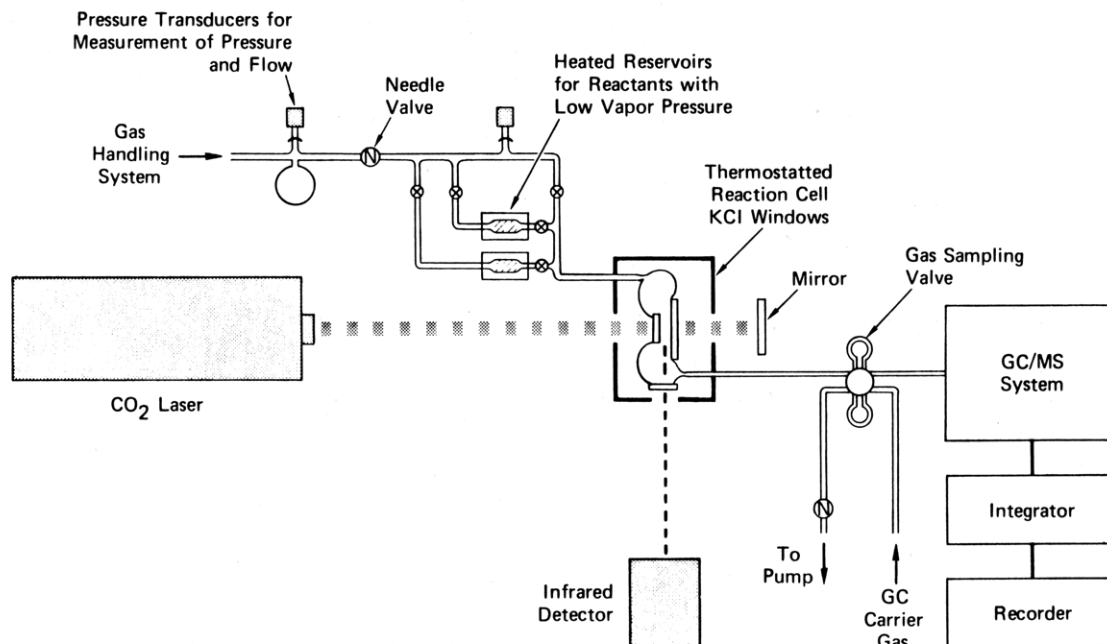


**Figure 1.** Schematic of gas chromatographically monitored laser-powered homogeneous pyrolysis flow system.

a sufficient number of these collisions, thermal equilibrium is attained, and observed reaction rates reflect thermal Arrhenius parameters. IR fluorescence measurements show that the entire mixture is brought to temperature in less than  $3 \mu\text{s}$  and that the reaction time before cooling by an expansion wave is about  $10 \mu\text{s}$ , far shorter than the millisecond time scale for diffusion to the walls. The heated flow system we have incorporated<sup>9</sup> makes this technique suitable for studying substrates (like the nitroaromatics) with very low vapor pressure at room temperature. This enables us to study the decomposition of the nitroaromatics under conditions where the rates and products of the initial step can be measured, and where a clear distinction can be made between homogeneous gas-phase processes and those processes aided by association with surfaces or condensed phases.

### Experimental Section

Figure 1 shows a schematic of the LPHP flow system, which is described in detail elsewhere.<sup>9</sup> A slow flow of  $\text{SF}_6$  (infrared absorber),  $\text{CO}_2$  (inert collider), temperature standard (cyclohexene), radical scavenger (*o*-fluorotoluene or cyclopentane), and substrate were passed through the reaction cell, through a heated gas chromatographic sampling valve, through a needle valve, and into a vacuum pump. The flow line and the reactor were heated to  $100^\circ\text{C}$ , to avoid condensation problems. Flow was maintained at the desired level by adjusting the first needle valve and total pressure was maintained at 110 torr by adjusting the second needle valve. A small portion of the reaction cell (typically 2–5%) was irradiated with the P20 line =  $10.6 \mu\text{m}$  of a Lumonics K103  $\text{CO}_2$  laser (duration =  $1 \mu\text{s}$ , fluence =  $1 \text{ J}/\text{cm}^2$ ) at a constant repetition rate (0.2 Hz) until a new steady state of products and undecomposed substrate was attained as shown schematically in Figure 2. The cell incorporates KCl windows to transmit the IR radiation, a  $1.2\text{-cm}^2$  laser aperture to define the heated volume, and a rear reflecting mirror to maintain axial temperature homogeneity under conditions where as much as 20% of the laser radiation is absorbed in a single pass. The reaction temperature was controlled by varying the IR radiation energy and the  $\text{SF}_6$  content of the gas mixture. The flow time and irradiation frequency provide at least 20 laser shots during the average flow lifetime of a substrate molecule in the cell and ensure complete gas mixing between shots.

When the system reaches the "steady-state" with the laser being repeatedly pulsed, the decrease in average concentration of sub-

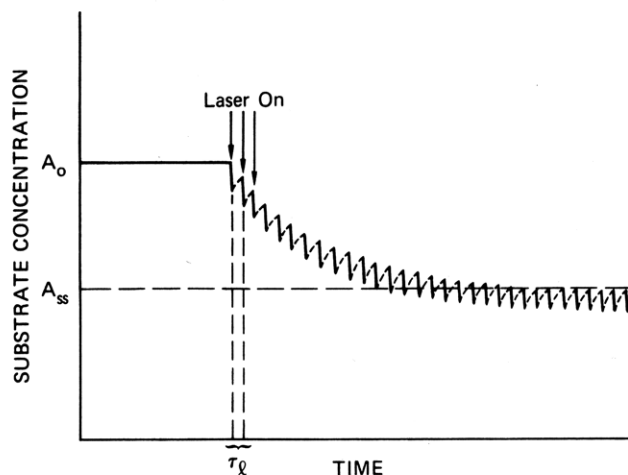


**Figure 2.** Schematic representation of a spatially averaged substrate concentration as a function of time.

strate A during any single laser pulse equals the replenishment (by flow) of A before the next laser pulse and results in the sawtooth horizontal line shown in Figure 2. Under these conditions, measurements of the average fractional decomposition lead to the rate constant for substrate decomposition via eq 1

$$k\tau_r \approx -\ln \left[ 1 - \left( \frac{[A]_0}{[A]_{ss}} - 1 \right) \frac{V_T}{V_R} \left( \frac{\tau_l}{\tau_F} \right) \right] \quad (\text{I})$$

where  $k$  is the first-order rate constant describing disappearance of A,  $\tau_r$  is the reaction time ( $10 \mu\text{s}$ ) following each laser pulse,  $\tau_l$  is the time between laser pulses (4 s),  $\tau_f$  is the flow lifetime in the reaction cell (typically 200 s),  $V_T$  and  $V_R$  are the total and laser-heated cell volumes, and  $A_0$  and  $A_{ss}$  are the laser-off and laser-on steady-state substrate concentrations, respectively.<sup>9</sup>

The need to measure explicitly the temperature corresponding to any particular measurement of  $k$  is eliminated by concurrent determination of the fractional decomposition of a temperature standard, a second substrate whose decomposition rate temperature dependence is already well-known, and therefore whose fraction decomposition defines an "effective" temperature.<sup>9</sup>

$\log k_1\tau_r =$

$$\log A_1 + \left( 1 - \frac{E_1}{E_2} \right) \log \tau_r - \frac{E_1}{E_2} \log A_2 + \frac{E_1}{E_2} \log k_2\tau_r \quad (\text{II})$$

(9) McMillen, D. F.; Lewis, K. E.; Smith, G. P.; Golden, D. M. *J. Phys. Chem.* **1983**, *86*, 709.

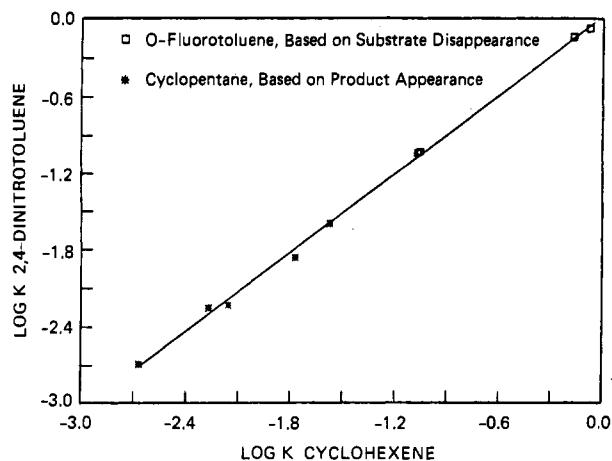


Figure 3. Effect of scavenger on 2,4-dinitrotoluene decomposition rate.

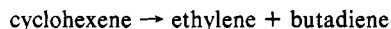
According to eq II, a plot of  $\log k_1$  vs.  $\log k_2$  gives a straight line of  $\log k_1 = \text{slope } E_1/E_2$  and intercept of

$$\log A_1 + [1 - (E_1/E_2)] \log \tau_r - [E_1/E_2] \log A_2$$

Inspection of eq II reveals that uncertainties in reaction times will cause no error in the slope of the comparative rate plot (the measured activation energy) and that the error in the intercept ( $A$  factor) will be given by  $[1 - (E_1/E_2)] \log(\tau_{r,\text{true}}/\tau_{r,\text{est}})$ . When  $E_1$  and  $E_2$  are not greatly different, this error will be insignificant. For example, when  $E_1/E_2 = 0.9$ , even a tenfold error in  $\tau_{r,\text{est}}$  will result in an error in  $\log A_{\text{meas}}$  of only 0.1 log units. This is in accord with the error analyses for the comparative rate technique as applied to the single-pulse shock tube.<sup>9,10</sup>

The comparative rate technique is similarly accommodating with respect to variations of temperature with time and space within the laser-heated volume. Under the conditions described above, and when the activation energy of the standard is within  $\sim 5$  kcal/mol of the unknown, and when the fractional decomposition of both unknown and standard are maintained below  $\sim 20\%$  per shot in the laser-heated volume, error analyses<sup>9,11</sup> and tests with "dummy" unknowns have shown<sup>9</sup> that the systematic error is less than  $\sim 1$  kcal/mol, irrespective of the range of the temperature variations. In other words, for suitably matched unknown and temperature standard, temperature variations will be tracked very similarly by the unknown and the standard. In the limit of exact Arrhenius parameter match, of course, there will be no systematic error.

Cyclohexene was chosen as the temperature standard because of its very well-known kinetic parameters, the stable products it forms, and also because its activation energy was close to the expected activation energies for the nitrocompounds.



$$\log k \text{ (s}^{-1}\text{)} = (15.15 - 66.6)/2.3RT$$

In all the experiments the products have been identified by using a GC equipped with a mass-selective detector (Hewlett Packard 5880 A and 5970 A) and the average concentrations of reactant and products were measured gas chromatographically by using a flame ionization detector.

## Results

For all of the nitroaromatics studied here the principal reaction pathway, as will be seen, involved scission of Ar-NO<sub>2</sub> bond to form, after radical scavenging, the corresponding Ar-H. Initial experiments, conducted without a radical scavenger, showed several secondary products in small amounts, so that the use of a scavenger to react with the radicals formed in the first step was necessary.

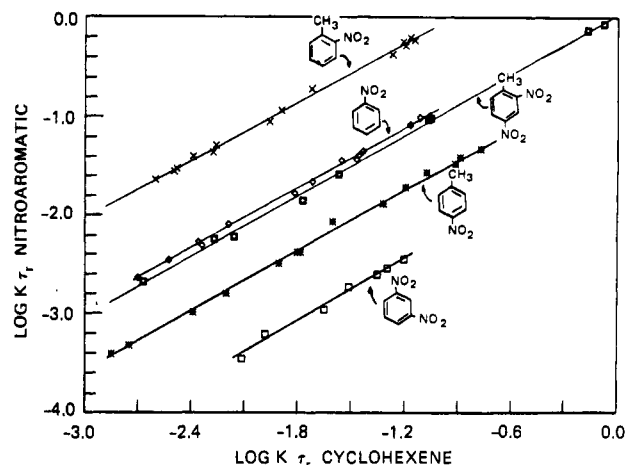


Figure 4. LPHP comparative rate plot for ArNO<sub>2</sub> decomposition.

TABLE I: LPHP Derived Arrhenius Parameters of Ar-NO<sub>2</sub> Decomposition

compd	$\log A_x$	$E_x$
NB <sup>a</sup>	$15.2 \pm 0.4$	$66.5 \pm 1.5$
<i>m</i> -DNB <sup>a</sup>	$14.5 \pm 0.5$	$70.0 \pm 2.1$
<i>p</i> -NT <sup>a</sup>	$14.8 \pm 0.5$	$67.8 \pm 2.0$
<i>o</i> -NT <sup>a</sup>	$15.9 \pm 0.5$	$65.5 \pm 2.0$
2,4-DNT <sup>a</sup>	$15.2 \pm 0.4$	$67.0 \pm 1.5$
NB <sup>b</sup>	$15.2 \pm 0.4$	$67.2 \pm 1.5$

<sup>a</sup>Rate parameters for total rate of Ar-NO<sub>2</sub> disappearance; the difference between these values and those for bond scission only is experimentally insignificant (i.e.,  $\Delta \log A \leq 0.04$ ). <sup>b</sup>Rate parameters for ArH formation only.

To choose the optimum amount of scavenger, several runs were made in the presence of *o*-fluorotoluene or cyclopentane up to a 400/1 ratio to the nitroaromatic concentration. When ratios greater than 50/1 were used, the system did not show any change in the reaction rate or in the product distribution. A ratio greater than 100/1 was usually used. Figure 3 shows a comparative rate plot for 2,4-DNT decomposition with *o*-fluorotoluene or cyclopentane as the radical scavenger, illustrating that the rate constants are independent of the identity of the scavenger.

Although small flow variations and low fractional decomposition make an exact mass balance difficult to establish, in only one case did the sum of all detected products leave more than 5–8% of the decomposed starting material unaccounted for. This was for *o*-nitrotoluene, where the mass balance ranged between 75 and 80%. Figure 3 shows a comparative rate plot for 2,4-dinitrotoluene that is based on starting material disappearance and product appearance, illustrating the good mass balance.

The comparative rate data plots for the decomposition of nitrobenzene to form benzene (75–80% yield based on the NB decomposed) and phenol (20–25%), *o*- and *p*-nitrotoluene to form toluene (70–95%) and *o*- and *p*-cresol, respectively (7–8%), 2,4-dinitrotoluene to form *p*-nitrotoluene and small amounts of *o*-nitrotoluene (8%), and *m*-dinitrobenzene to form nitrobenzene and small amounts of benzene are all shown in Figure 4.

The Arrhenius parameters ( $k_{\text{uni}}$ ) are obtained from the data in Figure 4 by using the comparative rate expression shown above (eq II). Since under the present conditions ( $p = 320\text{--}375$  torr and  $T = 1100\text{--}1250$  K), the cyclohexene decomposition is very slightly in the falloff ( $k_{\text{uni}}/k_{\infty} = 0.96\text{--}0.99$ ), the temperature dependence does not correspond exactly to the high-pressure Arrhenius parameters. In order to determine the temperature dependence of cyclohexene at this degree of falloff, we performed a RRKM calculation using a collision efficiency of  $\beta = 0.1\text{--}0.09$  and a transition-state model in which the motion of the separating fragments are treated as loosened vibrations. From this we derived

$$\log k_{\text{uni,CHE}} \text{ (s}^{-1}\text{)} = (14.9 - 65.5)/2.3RT$$

These parameters when coupled to the slope and intercept derived

(10) (a) Tsang, W. J. *Chem. Phys.* **1964**, *40*, 1171. (b) Tsang, W. J. *Ibid.* **1964**, *41*, 2487. (c) Tsang, W. J. *J. Phys. Chem.* **1972**, *76*, 143. (d) Tsang, W. J. *Ibid.* **1967**, *46*, 2817.

(11) Dai, H.-L.; Specht, E.; Berman, M. R.; Moore, C. B. *J. Chem. Phys.* **1982**, *77*, 4494.

**TABLE II: Experimental Parameters, Estimated Extents of Falloff, and High-Pressure Parameters for the Thermolyses of the Ar-NO<sub>2</sub> Bond**

compd	log $A_x$	$E_x$	derived high-pressure parameters		
			$k/k_\infty$	log $A_\infty$	$E_{a\infty}$
NB	15.2 ± 0.4	67.2 ± 1.5	0.84	15.5 ± 0.5	68.2 ± 1.7
1,3-DNB	14.5 ± 0.5	70.0 ± 2.1	(1)	14.5 ± 0.5	70.0 ± 2.1
<i>p</i> -NT	14.8 ± 0.5	67.8 ± 2.0	0.96	14.9 ± 0.5	68.2 ± 2.0
<i>o</i> -NT	15.9 ± 0.5	65.5 ± 2.0	0.75	16.4 ± 0.6	67.0 ± 2.2
2,4-DNT	15.2 ± 0.4	67.0 ± 1.5	0.96	15.3 ± 0.4	67.4 ± 1.7

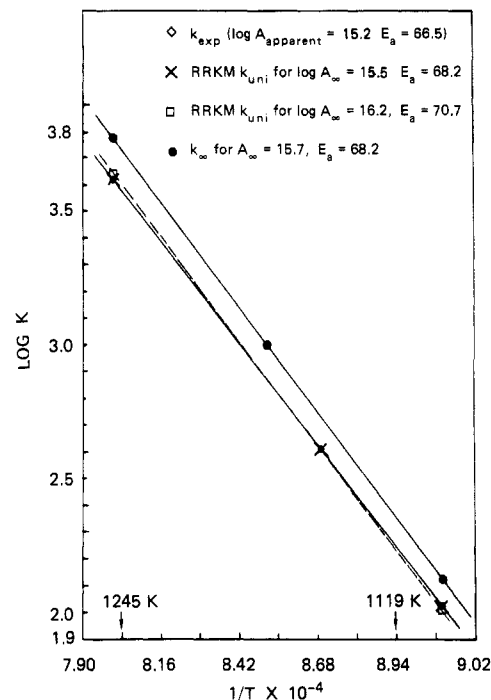
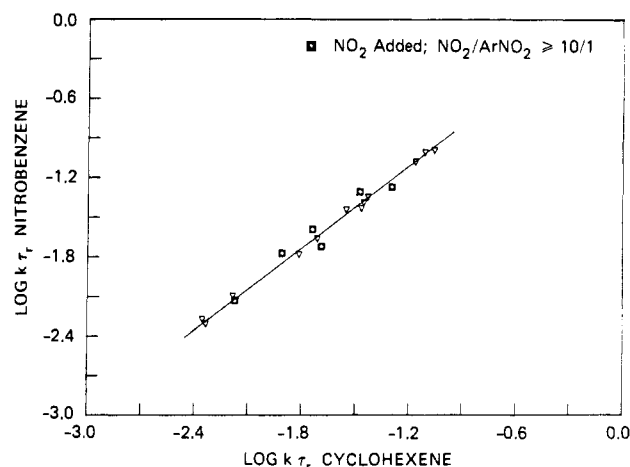
from the relative rate data plot give us the  $E_a$  and the  $A$  for the nitroaromatics summarized in Table I.

To obtain the high-pressure parameters, the experimental  $k_{uni}$  were fitted via an RRKM calculation using a modified Gorin model for the transition state<sup>12</sup> and literature vibrational assignments for nitrobenzene.<sup>13</sup> In this model the modes of the transition state are taken as the vibration and rotations of the NO<sub>2</sub> and phenyl fragments. The external rotation about the NO<sub>2</sub>-Ph axis is taken as active, and the other two external rotations are taken as adiabatic in the molecule. The internal rotation about the NO<sub>2</sub>-Ph axis is free in the transition state, and the other internal rotations of the phenyl and NO<sub>2</sub> fragments are taken as "restricted" free rotation at the Ph-NO<sub>2</sub> distance of the critical configuration. The degree of restriction is accounted for by the hindrance parameter<sup>12</sup> which ranged from 0.9 to 0.95, which decrease the entropy of the internal rotation by decreasing the effective moment of inertia of the rotor. A temperature-independent value 0.1 was chosen for the collision efficiency  $\beta$ . The results are presented in Tables II and III (virtually identical high-pressure Arrhenius parameters were obtained by fitting the data with a vibrational transition-state model). The changes in the nitrobenzene parameters that resulted from increasing  $\beta$  to 0.15 were negligible, mainly because the system is very close to the high-pressure limit.

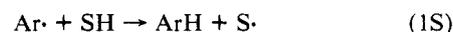
For each compound, we found the high-pressure parameters that best reproduced our experimental rate constants in the following way: we arbitrarily chose sets of  $A$  factors ranging from our  $A$  experimental to log  $A = 17.0$  at 0.5 log unit increments, (the high-pressure  $A$  factor was actually not constant, but was allowed to decrease by log  $A = 0.1$  from 1100 to 1250 K in order to match experimental curvature in log  $k$  vs.  $T$ . This corresponds to a slightly temperature-dependent value of the hindrance parameter.<sup>12</sup> We then adjusted  $E_c$  to fit our experimental rate constant at 1100 and 1250 K exactly. Unless the exactly correct  $A$  factors were by chance among those chosen initially, this required slightly different values of  $E_c$  at 1100 and 1250 K for each  $A$  factor. The best in the initially selected set of log  $A$  values was that which allowed the experimental  $k_{uni}$  to be fit exactly with a minimum difference in  $E_c$  at 1100 and 1250 K. We made the final adjustment by taking an  $E_c$  that is a weighted average of the set of values bracketing the correct  $E_c$  (i.e., the "minimum difference"  $E_c$  set), and with it obtained the high-pressure parameters that exactly reproduce the  $k_{uni}$  experimental at  $\bar{T}$ .

The question of the uniqueness of the rate parameters and the sensitivity of the fit is addressed by the Arrhenius plot in Figure 5. The solid line is a plot of  $k_{uni}(NB_{exptl})$  and also represents almost exactly the RRKM calculated  $k_{uni}$  values obtained for log  $A_\infty = 15.5$  (15.4 at 1250 K and  $E_\infty = 68.2$ . For comparison, the dashed  $k_{uni}$  values were calculated for log  $A_\infty = 16.2$  (16.1 at 1250 K). The upper solid line represents  $k_\infty$  for the fitted parameters, illustrating the extent of falloff observed under these conditions.

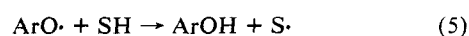
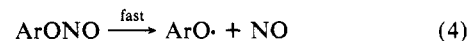
The above results provide convincing evidence that the homogeneous gas-phase thermal decomposition of the aromatic nitrocompounds in the presence of radical scavenger SH proceeds by initial homolysis of the C-NO<sub>2</sub> bond, the weakest in each of the respective substrates, and that the complex intramolecular steps

**Figure 5.** LPHP rate constants and RRKM fittings for nitrobenzene.**Figure 6.** Effect of NO<sub>2</sub> addition on nitrobenzene decomposition.

suggested in the literature do not take place as homogeneous gas-phase reactions:



In order to determine whether reaction 1 is reversible (-1) under the LPHP conditions, and to determine whether the observed phenol and cresol formation result from recombination of the NO<sub>2</sub> at the oxygen (-1') followed by reactions 4 and 5 or by an intramolecular rearrangement reaction 3, the decomposition of nitrobenzene was studied in the presence of added NO<sub>2</sub>.



Addition of NO<sub>2</sub> at ratios up to 50/1 NO<sub>2</sub>/NB did not affect either the product distribution or the rate parameters, as is shown in Figure 6. It is clear, therefore, that under the conditions of these experiments no Ar· returns either to ArNO<sub>2</sub> (-1) or to ArONO (-1'), and all observed phenol formation must be the

(12) Smith, G. P.; Golden, D. M. *Int. J. Chem. Kinet.* **1978**, *10*, 489.

(13) Green, J. H. S.; Harrison, D. J. *Spectrochim. Acta, Part A* **1970**, *26A*, 1925.

TABLE III: High-Pressure Arrhenius Parameters for Ar-NO<sub>2</sub> Homolysis and Derived BDE Values and Radical Recombination Parameters

compd	log <i>A</i> , s <sup>-1</sup>	<i>E</i> <sub>a</sub> , kcal/mol	BDE, <sup>a</sup> kcal/mol	Δ <i>S</i> <sub>d</sub> <sup>o, b</sup> cal/(mol °C)	log <i>A</i> <sub>r1100</sub> , s <sup>-1</sup> M <sup>-1</sup>	<i>E</i> <sub>a,r1100</sub> , <sup>c</sup> kcal/mol
NB	15.5 ± 0.5	68.2 ± 1.7	71.4 ± 2.0	45.5	8.6 ± 0.5	1.1
1,3-DNB	14.5 ± 0.5	70.0 ± 2.1	73.2 ± 2.4	42.3	8.4 ± 0.5	1.1
<i>p</i> -NT	14.9 ± 0.5	68.2 ± 2.0	71.4 ± 2.3	42.8	8.7 ± 0.5	1.1
<i>o</i> -NT	16.4 ± 0.6	67.0 ± 2.2	70.2 ± 2.5	49.6	8.7 ± 0.6	1.1
2,4-DNT	15.3 ± 0.4	67.4 ± 1.7	70.6 ± 2.0	42.8	8.7 ± 0.4	1.1

<sup>a</sup> Δ*H*<sub>298</sub><sup>o</sup>. <sup>b</sup> For the sake of consistency, the lower bond scission *A* factors have been taken to imply lower overall entropy decreases for dissociation. This results in a compensation effect, making all log *A*<sub>r</sub> similar. <sup>c</sup> *E*<sub>a</sub> is for recombination described in concentration units.

TABLE IV: Effect of Substituents

compd	log <i>k</i> <sub>∞</sub> (1100 K) <sup>a</sup>	ΔBDE, kcal/mol	Δ log <i>k</i>	Δ(Δ <i>G</i> <sup>o</sup> ), <sup>b</sup> kcal/mol
NB	1.93	(0)	(0)	(0)
<i>m</i> -DNB	0.59	+1.8	-1.34	+6.7
<i>p</i> -NT	1.32	0	-0.61	+3.1
<i>o</i> -NT	3.03	-1.2	1.10	-5.5
2,4-DNT	1.91 <sup>c</sup>	-0.8 <sup>d</sup>	-0.02	+0.1

<sup>a</sup> These values are taken from the RRKM fitting of the measured rate constants, and differ slightly from the "raw" data plotted in Figure 4. <sup>b</sup> (Δ log *k*)(2.3*RT*<sub>1100</sub>). <sup>c</sup> Predicted log *k*(1100; 2,4-DNT) = 1.97 + 1.10 - 1.34 = 1.69. <sup>d</sup> Predicted ΔBDE(2,4-DNT) = 1.8 - 1.2 = +0.6.

result of an intramolecular process 3. This does not imply that under no conditions can phenol formation result from phenyl-NO<sub>2</sub> recombination; these results only show that it does not result under LPHP conditions, where the ratios of scavenger to phenyl radicals and scavenger radicals to phenyl radicals are so large that NO<sub>2</sub> is consumed either by abstracting hydrogen from the scavenger or by oxidizing the scavenger radicals, but not by oxidizing the phenyl radicals (reactions -1' and 4).

The high-pressure rate parameters associated with reaction 1 are shown in Table III. From these parameters the bond dissociation energies for Ar-NO<sub>2</sub> and the Arrhenius parameters for the recombination reaction at 1100 K have been calculated, assuming an unhindered Gorin model<sup>12</sup> for the transition state (see above), and are also shown in that table. The BDE we have obtained for nitrobenzene (71.4 kcal/mol) is in very good agreement with the value of 71.3 kcal/mol selected by McMillen and Golden.<sup>5b</sup> From the BDE values for the removal of the NO<sub>2</sub> from *p*-nitrotoluene and 2,4-dinitrotoluene and their heats of formation,<sup>14</sup> the heats of formation of CH<sub>3</sub>-Ph and CH<sub>3</sub>-Ph-NO<sub>2</sub> are determined to be 70.9 and 71.1 kcal/mol, using the thermodynamic relationship Δ*H*<sub>f</sub><sup>o</sup><sub>298</sub>(Ph) = Δ*H*<sub>f</sub><sup>o</sup><sub>298</sub>(Ph-NO<sub>2</sub>) + BDE(Ph-NO<sub>2</sub>) - Δ*H*<sub>f</sub><sup>o</sup><sub>298</sub>(NO<sub>2</sub>). The rate parameters associated with the reaction of nitrobenzene forming NO (i.e., nitric oxide) and phenol have been determined as log *k*<sub>∞</sub> (s<sup>-1</sup>) = (14.3 ± 1.0) - (65.5 ± 5)/2.3*RT*.

## Discussion

We have carefully chosen a set of nitroaromatic compounds that allows us to determine the effect of methyl and NO<sub>2</sub> substitution on their kinetic behavior. As described above, in all cases the principal initial step is Ar-NO<sub>2</sub> bond scission. The effects of the various substitution on the rate of this step are compared in Table IV. These effects are clearly quite self-consistent and appear to be additive. This can be seen by summing the observed log *k* values for the NB and *m*-DNB, and NB and *o*-NT, to predict the log *k* value for the ArNO<sub>2</sub> which has both a *m*-NO<sub>2</sub> and an *o*-methyl substituent. The agreement between the predicted and measured values is essentially exact. Similarly, the rate constants reported here for NB (forming benzene and phenol) are in very good agreement with those recently measured by Tsang in a heated single-pulse shock tube,<sup>15</sup> log *k* (s<sup>-1</sup>) = (15.4 - 66.0)/2.3*RT*.

For *o*-NT, on the other hand, preliminary results of Tsang are in some disagreement with those presented here. Although the

absolute rates of *o*-NT decomposition are very similar, the yield of toluene in the heated shock tube is apparently substantially less than the 70-75% observed in the LPHP system, and no other products are detected by the GC. Tests by Tsang to determine whether the shortage of gas-phase products reflects a difference in the initial *o*-NT decomposition reaction or a difference in the scavenging of the initially formed radical have not yet provided a conclusive answer, but a good mass balance of the expected products is observed with *p*-NT.

The identification of the toluene we report in 70-75% yield is certain: the retention time is coincident with (i.e., varies 0.005 min from) that of authentic toluene spiked into the product mixture, and the mass spectrum of that GC peak confirms it as toluene. Cyclohexatriene is a possible product, particularly since ESR studies have implicated, in condensed-phase decomposition, formation of a radical with five protons having equivalent coupling to the radical center, such as would be produced by rearrangement of an initial dinitrophenyl radical to a dinitrocyclohexatrienyl radical. In the present work, cyclohexatriene is ruled out by a retention time difference of 0.35 min, even though as an isomer of toluene it is mass spectrometrically similar.

In addition to agreement on absolute rates, there is some "qualitative" agreement between our results for *o*-NT and those of Tsang, in that our 70-75% yield of toluene is poorer than the 90-95% observed for all the other Ar-NO<sub>2</sub> studied here, and we were not able, by varying pyrolysis conditions (e.g., laser beam intensity, scavenger identity, pressure, etc.), to raise the yield beyond ~75% of the *o*-NT decomposed. On the other hand, with *p*-NT and 2,4-DNT, which has the same *o*-methyl relationship with one of its NO<sub>2</sub> groups, our mass balance was 90% or better, and there was not even a hint of a tendency to undergo a reaction other than Ar-NO<sub>2</sub> scission (or ArOH formation).

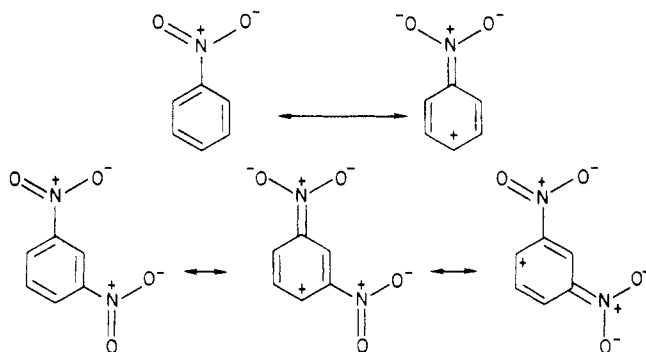
In light of this puzzling behavior of *o*-NT, it may be useful to examine the observed effects of methyl and NO<sub>2</sub> substitution on the Ar-NO<sub>2</sub> homolysis kinetics. The BDE values in Table I, as discussed above, are based upon the measured values for the temperature dependence, taken at face value. The stated error limits are random error limits (one standard deviation), determined largely by the scatter in the comparative rate plots. The data provide no firm basis for choosing either activation energies or absolute rates as the preferred indicator of relative BDE values. Given random error limits and the well-known susceptibility of Arrhenius plots to unforeseen systematic errors, the significant point is that the measured absolute rates reflect substituent effects that are additive and thus would seem to constitute a set of very self-consistent data. That is, the effect on decomposition rate of a *m*-NO<sub>2</sub> substituent is the same on going from NB to *m*-DNB as it is in going from *o*-NT to 2,4-DNT (Table IV). Beyond the self-consistency in absolute rates, there are certain trends in the data that suggest the least-squares intercepts and slopes correctly indicate, in most cases, whether the measured rate constants differences are due to activation energy or *A* factor differences.

Examination of the rate parameters we have obtained for the nitroaromatics (Tables III and IV) suggests that the changes in the rate constants reflect mainly *A* factor changes. Thus the high value for *o*-NT presumably arises from the greater decreases in the barrier to internal rotation of the methyl and NO<sub>2</sub> groups and from some relief of angle strain as the NO<sub>2</sub> departs, as compared with the reaction of nitrobenzene itself or with *p*-NT. The lower rates for *m*-DNB and 2,4-DNT are associated with slightly higher BDE values (and activation energies) and substantially lower *A*

(14) Lenchitz, C.; Velicky, R. W.; Sikvestro, G.; Schlosberg, L. P. *J. Chem. Thermodyn.* 1971, 3, 689.

(15) Tsang, W., private communication.

factors. Although a slightly tighter transition state (lower  $A$  factor) would be expected with a stronger bond, the large apparent drop in the  $A$  factors cannot be rationalized on that basis alone. An observed  $\Delta \log A = 1.0$  in going from NO to *m*-DNO could be easily ascribed to random errors in the Arrhenius parameters, were it not for the fact that this  $A$  factor drop is almost exactly duplicated in going from *o*-NT to 2,4-DNT. A possible rationalization lies in the fact that a second NO<sub>2</sub> meta to the first decreases the importance of C-N double-bonded resonance structures involving any one of the NO<sub>2</sub> groups.



This "inhibition" will decrease as one of the -NO<sub>2</sub> groups departs, allowing more contribution of a C-N double-bond structure for the remaining -NO<sub>2</sub> group. This will result in an increase in the barrier to internal rotation and a consequent decrease in the  $A$  factor because of the lower rotational entropy of the transition state. (It should be noted that the lower bond-scission  $A$  factors in Table III, have been taken to imply lower overall entropy increases for dissociation. This results in a "compensation" such that all recombination  $A$  factors are similar (i.e.,  $10^{8.5} \pm 0.2$ .)

In the case of *p*-NT, the decrease in rate of decomposition (as compared to NB) is suggested by the Arrhenius parameters to be due entirely to a lower  $A$  factor. In contrast, we would have expected similar  $A$  factors for *p*-NT and NB (since the methyl in the para position should have little impact on relief of strain), and we would have expected the decrease in rate with *p*-methyl substitution to result from a slight strengthening of the Ar-NO<sub>2</sub> bond, rationalizable in terms of inductive stabilization of contributing structures that contain a C-N double bond. In fact, however, the activation-energy-based BDE for *p*-NT is the same as for *o*-NT (though a BDE difference sufficient to cause the observed rate differences would be, at  $\sim 3.3$  kcal/mol, easily within combined standard deviations for the two activation energies) and the rate difference is reflected in a lower  $A$  factor.

The important point is that the rate difference between *p*-NT and *o*-NT (where in the absence of steric effects we would expect little electronic effect) amounts to a difference in free energy of activation of 9 kcal/mol. Thus, even though our results demonstrate that phenyl-NO<sub>2</sub> bonds scission remains the principal

rate-limiting step when an *o*-methyl group is present, the methyl group clearly gives a substantial "push" to the departing NO<sub>2</sub> group. This would seem to be a situation in which some outside influence (e.g., contact with solid surfaces or condensed phases) could trigger some reaction in which one of the hydrogens of the methyl group "pushes" all the way into the nitro group, ultimately transferring a hydrogen to the nitrogen. In other words, the present results indicating Ph-NO<sub>2</sub> bond scission substantially accelerated by an *o*-methyl group show that the strong methyl-NO<sub>2</sub> interaction has not, for an isolated Ar-NO<sub>2</sub> molecule, yet reached the threshold for some different reaction. However, it may be that the extent of "outside" interferences necessary to bring about such a change in *o*-nitrotoluenes is not very great. The nearness of this threshold could be responsible both for the missing products in the shock tube decomposition<sup>15</sup> and for the anomalous behavior of nitrotoluenes reported in the literature.<sup>2,4,6,7</sup> The present results, however, demonstrate that these anomalous effects account, at most, for 25% of the decomposition of nitrotoluene isolated gas-phase molecules at temperatures in the range of 900-1000 °C, and that additional factors must be brought into play in order to open up a new reaction channel that can compete with homolysis of the Ar-NO<sub>2</sub> bond. Having made this determination for mono- and dinitrotoluenes, the question of whether the decomposition of isolated trinitrotoluene molecules also proceeds by C-NO<sub>2</sub> bond scission is now being addressed in our laboratory. Once the behavior of isolated gas-phase molecules is characterized also for trinitrotoluene, then the question of intermolecular interactions that bear on the functioning and malfunctioning of these and similar energetic materials can be addressed.

The effects of methyl and NO<sub>2</sub> substitution on phenyl-NO<sub>2</sub> bond cleavage (Table IV) can be summarized in terms of the effect on the activation-energy-based BDE values on the free energy of activation. The latter approximates the change in BDE if all  $A$  factors were assumed to be equal: (a) *m*-NO<sub>2</sub> substitution increases the phenyl-NO<sub>2</sub> BDE by 2 kcal/mol and  $\Delta G^*$  by 6.7 kcal/mol; (b) *p*-Me substitution (where there is no steric effect) does not show any effect on the activation-energy-based phenyl-NO<sub>2</sub> BDE, but slows the bond scission rate by a factor of 5 (and therefore raises  $\Delta G^*$  by 3.1 kcal/mol); (c) for *o*-Me substitution, any electronic effect is overwhelmed by a steric effect, resulting in a net decrease in BDE of 1 kcal/mol and a substantially higher  $A$  factor; (d) when the molecule has both *m*-NO<sub>2</sub> and *o*-Me substitution, the bond-strengthening and bond-weakening effects roughly cancel.

**Acknowledgment.** We acknowledge the support of this work by the U.S. Army Research Office, Contract No. DAAG29-82-K-0169. We appreciate helpful discussions with W. Tsang and the communication of his results prior to publication.

**Registry No.** NB, 98-95-3; *m*-DNB, 99-65-0; *p*-NT, 99-99-0; *o*-NT, 88-72-2; 2,4-DNT, 121-14-2; 1,3-DNT, 99-65-0; NO<sub>2</sub>, 10102-44-0.